

Hall effect, magnetization and conductivity of Fe_3O_4 epitaxial thin films

D. Reisinger,* P. Majewski, M. Opel, L. Alff, and R. Gross
*Walther-Meißner-Institut, Bayerische Akademie der Wissenschaften,
 Walther-Meißner Str. 8, 85748 Garching, Germany*
 (Dated: received April 5, 2004)

Magnetite epitaxial thin films have been prepared by pulsed laser deposition on MgO and Si substrates. The magnetic and electrical properties of these epitaxial films are close to those of single crystals. For 40 - 50 nm thick films, the saturation magnetization and electrical conductivity are $\sim 450 \text{ emu/cm}^3$ and $225 \Omega^{-1}\text{cm}^{-1}$ at room temperature, respectively. The Verwey transition temperature is 117 K. The Hall effect data yield an electron concentration corresponding to 0.22 electrons per formula unit at room temperature. Both normal and anomalous Hall effect have been found to have negative sign.

PACS numbers: 72.15.-v 72.80.Ga 75.70.-i

Half-metallic materials with 100% spin polarization of the charge carriers at the Fermi-level are under intensive investigation due to their potential application in spintronics. Promising candidates with theoretically predicted half-metallicity are Fe_3O_4 ¹, CrO_2 ², Mn based Heusler alloys³, doped manganites⁴, and double perovskites^{5,6} with magnetite having the highest Curie temperature ($T_C \simeq 850 \text{ K}$). Also, magnetite has a low magnetic-crystalline anisotropy. For the use of magnetite in spintronic devices, the growth of high quality thin films is required. Recently, Fe_3O_4 thin films have been grown by different techniques including sputtering⁷, molecular beam epitaxy⁸ and pulsed laser deposition^{9,10} on various substrates (MgO, MgAl_2O_4 , SrTiO_3 , sapphire, and Si). On Si, epitaxial thin films can be grown despite the large lattice mismatch using a suitable buffer layer system, for example a combination of TiN and MgO¹¹. In this letter, we report electrical transport, magnetization, and Hall effect measurements on high quality epitaxial magnetite thin films grown on MgO and Si substrates by laser molecular beam epitaxy¹². The key result is, that for the high quality epitaxial films about the same properties can be achieved as for bulk samples. In particular, we report on Hall effect measurements showing that the magnetite thin films have a similar charge carrier concentration at room temperature as single crystals¹³. To the best of our knowledge, there is at present no other Hall measurement available for magnetite thin films.

The typically 40 to 50 nm thick manganite thin films were deposited from a stoichiometric target by laser molecular beam epitaxy¹² at a substrate temperature of 340°C on MgO(001) or Si(001) substrates. In-situ RHEED was used to monitor the block-by-block growth mode^{12,14} of magnetite. Note that for Fe_3O_4 four RHEED intensity oscillations are observed per unit cell¹⁵ corresponding to four charge neutral blocks of composition $\text{Fe}(\text{A})_2^{3+}\text{Fe}(\text{B})_2^{3+}\text{Fe}(\text{B})_2^{2+}\text{O}_8^{2-}$. Here, A and B refer to the tetrahedral and octahedral sites of the inverse spinel structure, respectively, where the B-site is equally occupied by Fe^{3+} and Fe^{2+} ions. A more detailed discussion of the thin film growth process on Si is given in Ref.¹¹. In order to prevent surface oxidation, the mag-

netite films were covered by an about 10 nm thick MgO cap layer. X-ray analysis gives a Fe_3O_4 *c*-axis value of 8.39 Å and a typical mosaic spread of 0.02° for MgO substrates. No impurity phases, for example from other iron oxides, could be observed in the diffraction pattern. The rms surface roughness as determined by AFM had typical values ranging between 2 and 5 Å averaged over an area of $1 \mu\text{m}^2$. The film thickness was evaluated by counting the RHEED intensity oscillations and verified by x-ray reflectometry.

In Fig. 1, the electrical conductivity σ of an epitaxial Fe_3O_4 thin film grown on a MgO(001) symmetrically [001] tilt bicrystal substrate with a misorientation angle of 24.8° degree is plotted versus $1/T$. From this data we can conclude the following: First, it is evident that the $\sigma(T)$ curve obtained for a bridge straddling the grain boundary is the same as for bridges containing no grain boundary. That is, obviously the grain boundary resistance is much smaller than the resistance of the adjacent film part of the bridge. A similar effect has been observed for grain boundaries in doped manganites, where only a high-temperature annealing process in oxygen atmosphere produces a grain boundary with sufficiently high resistance¹⁹. Second, the absolute value of the conductivity of about $225 \Omega^{-1}\text{cm}^{-1}$ at room temperature is comparable to the best values of about $250 \Omega^{-1}\text{cm}^{-1}$ reported for bulk samples¹⁶ and of about $190 \Omega^{-1}\text{cm}^{-1}$ reported for films of the same (50 nm) thickness¹⁷. Recently, a decrease of σ has been reported for films thinner than 50 nm¹⁷ due to a decrease of the antiphase domain size. However, there are also reports that the conductivity does not change down to 10 nm¹⁸. Third, the Verwey transition at $T_V \simeq 120 \text{ K}$ appears smeared out in the $\sigma(T)$ curve as compared to single crystals, where a sharp jump in $\sigma(T)$ is observed. We note that also the magnetic moment (see inset in Fig. 1) gradually decreases starting already above 150 K. This is again in contrast to bulk samples, where a sharp jump is observed at T_V . However, the data clearly shows a sharp kink structure at $T_V = 117 \text{ K}$. The physics of this Verwey transition and its relation to a possible charge order is still under discussion.

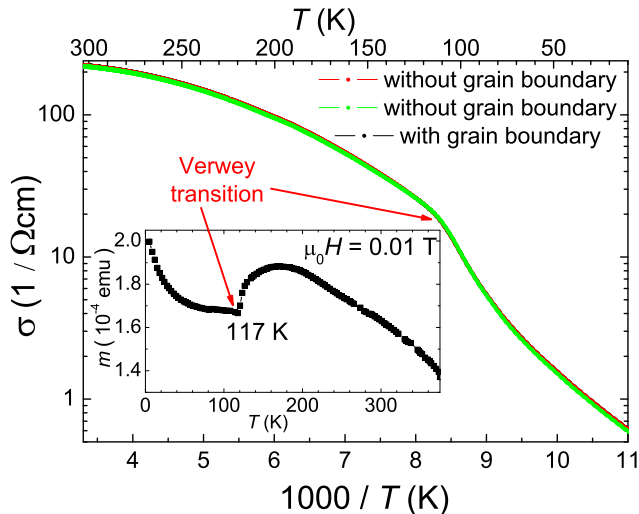


Figure 1: Electrical conductivity of a 45 nm thick epitaxial Fe_3O_4 films grown on a MgO bicrystal plotted versus $1/T$. The curves for bridges with and without grain boundary are indistinguishable. The Verwey transition around 120 K can be best seen in the inset, where magnetic moment measured in a field of 100 Oe is plotted vs. temperature.

Fig. 2 shows the magnetization vs applied field dependencies for Fe_3O_4 films grown on MgO and Si¹¹. At 300 K, the saturation magnetization M_s is about 3.6 and $3.5 \mu_B/\text{f.u.}$ for the film on MgO and Si, respectively. At 150 K, this value increases to $3.8 \mu_B/\text{f.u.}$. The coercive field is about 30 mT at room temperature. The magnetization data show that the M_s values of our epitaxial films with a thickness ranging between 40 and 50 nm are close to the theoretically expected bulk value of $M_s = 4 \mu_B/\text{f.u.}$. Our M_s values are among the highest reported for thin films in the literature so far^{7,18,20}. We also note that our room temperature M_s value of $453 \text{ emu}/\text{cm}^3$ is close to the value of $471 \text{ emu}/\text{cm}^3$ reported for a single crystal²¹, i.e. for our thin films about 96% of the bulk value is reached. We attribute the high M_s values of our films their good structural properties of the films and the fact that surface oxidation is prevented using a MgO cap layer. Due to the good lattice match between the film and the substrate (for the Si substrate the lattice mismatch is relaxed using a TiN/MgO double buffer layer system¹¹) also strain effects play no important role.

In Fig. 3, the Hall resistivity is plotted versus the applied magnetic field at $T = 290 \text{ K}$. It is well known that in nonmagnetic metals the familiar Hall current arises when electrons moving in crossed electric (\mathbf{E}) and magnetic fields (\mathbf{H}) are deflected by the Lorentz force. However, in a ferromagnet subject to \mathbf{E} alone, an anomalous Hall current appears transverse to \mathbf{E} . Karplus and Luttinger²² proposed a quantum mechanical origin of the Hall current, where an electron in the conduction band spends part of its time in nearby bands thereby acquiring a spin-dependent anomalous velocity. In modern terms,

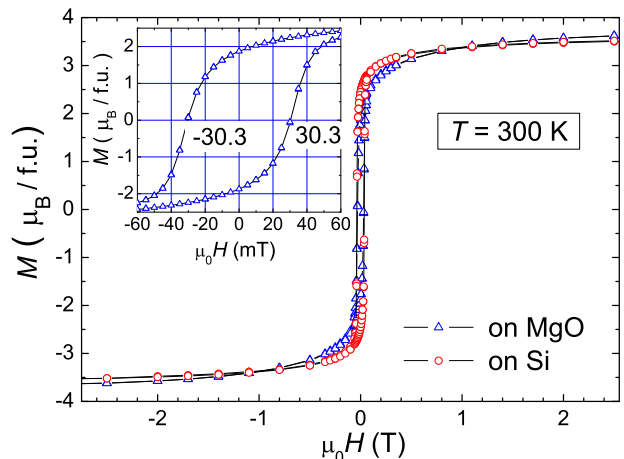


Figure 2: Magnetization versus applied magnetic field at 300 K for epitaxial Fe_3O_4 films grown on MgO and Si substrates. The field was applied in-plane. The inset shows a blowup of the low field part of the hysteresis curve for the film grown on MgO.

this anomalous velocity is related to the Berry phase and recently has been applied to explain the anomalous Hall effect (AHE) in Mn-doped GaAs²³. A more conventional explanation is based on skew scattering and side jump²⁴. Unfortunately, the anomalous Hall effect in itinerant ferromagnets is still discussed controversially. In an AHE experiment the observed Hall resistivity ρ_H comprises two terms,

$$\rho_H = R_0 \mu_0 H + R_A \mu_0 M, \quad (1)$$

where R_0 is the ordinary and R_A the anomalous Hall coefficient. It is evident that after the magnetization M has saturated on increasing the applied field H , the *change* of ρ_H is only due to the normal Hall effect. From the linear high field dependence of the Hall effect data we derive $R_0 \simeq -2.12 \cdot 10^{-9} \text{ m}^3/\text{C}$ at 300 K. With the relation $R_0 = 1/en$ we obtain the electron density $n = 2.95 \cdot 10^{21} / \text{cm}^3$. With the density $\rho = 5.185 \text{ g}/\text{cm}^3$ we then obtain the number of electrons per Fe_3O_4 formula unit to 0.22. This value is comparable to that observed in bulk single crystal samples¹³. The negative sign of the ordinary Hall coefficient suggests electron conduction. We also note that R_0 is slightly larger at 160 K as compared to 300 K due to the increase in the Hall mobility. The Hall mobility μ_H is given by the product of the ordinary Hall coefficient and the conductivity. At 300 K we obtain $\mu_H \simeq 0.48 \text{ cm}^2/\text{Vs}$. The anomalous Hall coefficient at 300 K is determined to $R_A \simeq -2.5 \cdot 10^{-7} \text{ m}^3/\text{As}$ using the measured saturation magnetization of $3.6 \mu_B$ per formula unit. We note that in the half-metallic double perovskite $\text{Sr}_2\text{FeMoO}_6$ R_A shows a positive sign, while R_0 is negative²⁵. This is in contrast to magnetite, where both R_0 and R_A have negative sign. Within a simple model the different signs of R_A for different materials can be understood in terms of asymmetric scattering due

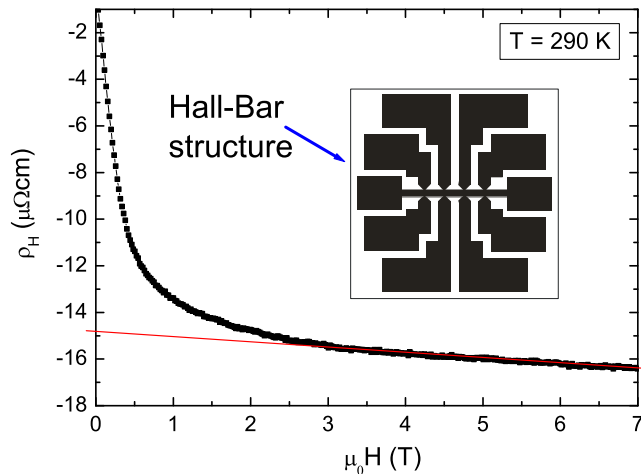


Figure 3: Hall effect for a Fe_3O_4 thin film grown on (001) MgO . The dotted line is a fit to the high field data, where the film magnetization saturates. The inset shows an optical micrograph of the Hall bar geometry.

to different densities of states available for positive and negative orbital orientations²⁶.

Discussing σ and n we can state that in a simple physical picture one would expect that the minority spin electron that is shared by the two octahedrally coordinated

B-sites gives rise to electronic conductivity above the Verwey transition. Below the Verwey transition, charge ordering of the B-site ions leads to an insulating state. However, the physical picture of charge ordering below the Verwey transition has been challenged for example by resonant x-ray scattering measurements²⁷. The observation that only 0.22 electrons per f.u. contribute to the conductivity could be explained by localization effects due to electronic correlations. Recently, in an *ab initio* study of charge order in magnetite the local spin density has been calculated as a function of symmetry (or structural distortion). This calculation yields 100% spin polarization, a total spin magnetic moment of about $4.0 \mu_B$ and about 0.24 electronic states per formula unit at the Fermi level²⁸. Although these values have been calculated for the charge ordered ground state, they are remarkably consistent with the results obtained in our study above the Verwey transition.

In summary, we have grown high quality epitaxial thin films of magnetite with properties comparable to those of best bulk samples. For the first time, we report Hall effect measurements for thin films, indicating that only 0.22 electrons per formula unit contribute to electrical conductivity.

This work was supported by the Deutsche Forschungsgemeinschaft (Al/560) and the Bundesministerium für Bildung und Forschung (project 13N8279).

* Electronic address: Daniel.Reisinger@wmi.badw.de

¹ Z. Zhang and S. Satpathy, Phys. Rev. B **44**, 13319 (1991).

² M. A. Korotin, V. I. Anisimov, D. I. Khomskii, and G. A. Sawatzky, Phys. Rev. Lett. **80**, 4305 (1998).

³ R. A. de Groot, F. M. Mueller, P. G. van Engen, and K. H. J. Buschow, Phys. Rev. Lett. **50**, 2024 (1983).

⁴ W. E. Pickett and D. J. Singh, Phys. Rev. B **53**, 1146 (1996).

⁵ K.-I. Kobayashi, T. Kimura, H. Sawada, K. Terakura, and Y. Tokura, Nature (London) **395**, 677 (1998).

⁶ J. B. Philipp, P. Majewski, L. Alff, A. Erb, R. Gross, T. Graf, M. S. Brandt, J. Simon, T. Walther, W. Mader, D. Topwal, and D. D. Sarma, Phys. Rev. B **68**, 14???? (2003).

⁷ D. T. Margulies, F. T. Parker, F. E. Spada, R. S. Goldman, J. Li, R. Sinclair, and A. E. Berkowitz, Phys. Rev. B **53**, 9175 (1996).

⁸ F. C. Voegt, T. T. M. Palstra, L. Niesen, O. C. Rogojuanu, M. A. James, and T. Hibma, Phys. Rev. B **57**, 8107(R) (1998).

⁹ G. Q. Gong, A. Gupta, G. Xiao, W. Qian, and V. P. Dravid, Phys. Rev. B **56**, 5096 (1997).

¹⁰ S. B. Ogale, K. Ghosh, R. P. Sharma, R. L. Greene, R. Ramesh, and T. Venkatesan, Phys. Rev. B **57**, 7823 (1998).

¹¹ D. Reisinger, M. Schonecke, T. Brenninger, M. Opel, A. Erb, L. Alff, and R. Gross, J. Appl. Phys. **94**, 1857 (2003).

¹² R. Gross, J. Klein, B. Wiedenhorst, C. Höfener, U. Schoop, J. B. Philipp, M. Schonecke, F. Herbstritt, L. Alff, Yafeng Lu, A. Marx, S. Schymon, S. Thienhaus, W. Mader, in *Superconducting and Related Oxides: Physics and Nanoengineering IV*, D. Pavuna and I. Bosovic eds., SPIE Conf. Proc. **Vol. 4058** (2000), pp. 278–294.

¹³ J. M. Lavine, Phys. Rev. **114**, 482 (1959).

¹⁴ J. Klein, C. Höfener, L. Alff, and R. Gross, Supercond. Sci. Technol. **12**, 1023 (1999); see also

J. Magn. Magn. Mater. **211**, 9 (2000).

¹⁵ D. Reisinger, B. Blass, J. Klein, J. B. Philipp, M. Schonecke, A. Erb, L. Alff, and R. Gross, Appl. Phys. A **77**, 619 (2003).

¹⁶ B. A. Calhoun, Phys. Rev. **94**, 1577 (1954).

¹⁷ W. Eerenstein, T. T. M. Palstra, T. Hibma, and S. Celotto, Phys. Rev. B **66**, 201101(R) (2002).

¹⁸ S. Soeya, J. Hayakawa, H. Takahashi, K. Ito, C. Yamamoto, A. Kida, H. Asano, and M. Matsui, Appl. Phys. Lett. **80**, 823 (2002).

¹⁹ J. B. Philipp, C. Höfener, S. Thienhaus, J. Klein, L. Alff, and R. Gross, Phys. Rev. B **62**, 9248(R) (2000).

²⁰ S. Kale, S. M. Bhagat, S. E. Lofland, T. Scabarozzi, S. B. Ogale, A. Orozco, S. R. Shinde, T. Venkatesan, B. Hannoyer, B. Mercey, and W. Prellier, Phys. Rev. B **64**, 205413 (2001).

²¹ *Magnetic and other properties of oxides and related compounds*, edited by K.-H. Hellwege and A. M. Hellwege, Landolt-Börnstein, New Series, Group III, Vol. 4, Pt. b (Springer-Verlag, Berlin, 1970).

²² R. Karplus, J. M. Luttinger, Phys. Rev. **95**, 1154 (1954); J. M. Luttinger, Phys. Rev. **112**, 739 (1958).

²³ T. Jungwirth, Q. Niu, and A. H. MacDonald, Phys. Rev. Lett. **88**, 207208 (2002).

²⁴ P. Nozières, C. Lewiner, J. Phys. (France) **34**, 901 (1973).

²⁵ W. Westerburg, D. Reisinger, and G. Jakob, Phys. Rev. B **62**, 767(R) (2000).

²⁶ A. Fert, O. Jaoul, Phys. Rev. Lett. **28**, 303 (1972).

²⁷ J. García, G. Subías, M. G. Proietti, J. Blasco, H. Renevier, J. L. Hodeau, and Y. Joli, Phys. Rev. B **63**, 054110 (2001).

²⁸ Z. Szotek, W. M. Temmermann, A. Svane, L. Petit, G. M. Stocks, and H. Winter, Phys. Rev. B **68**, 054415 (2003).